A.

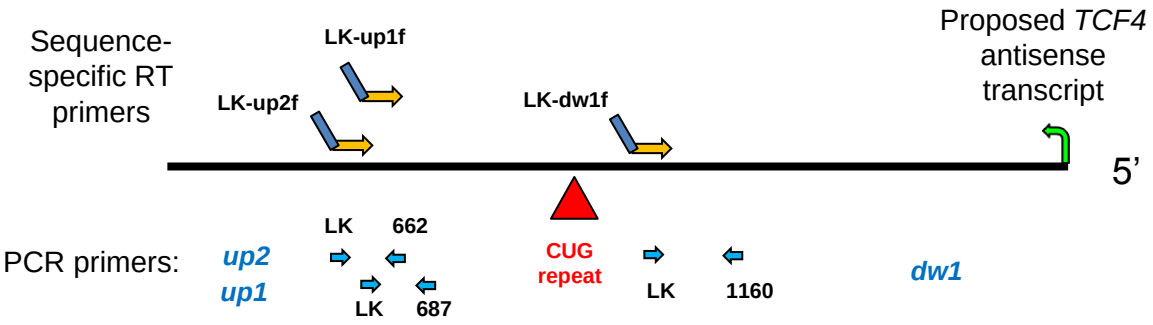

B.

Primer	Sequence (5'-3')
LK	CGACTGGAGCACGAGGACACTGA
LK-up1	CGACTGGAGCACGAGGACACTGATGTGG AGTTTTACGGCTGTA
LK-up2	CGACTGGAGCACGAGGACACTGAGTAGT CGTAGGATCAGCACAAAG
LK-dw1	CGACTGGAGCACGAGGACACTGACACTT TCTCCATTCGTTCCTTTG
up1	R: ATGTCTGGGACTTGGTTTAGG
up2	R: GGAAGCAAAGGGATGGAGAA
dw1	R: TCTCTCTTTCACTCCCTCTCTC

C.

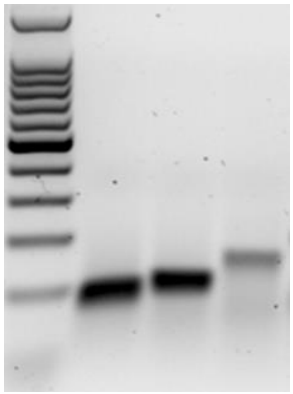

D.

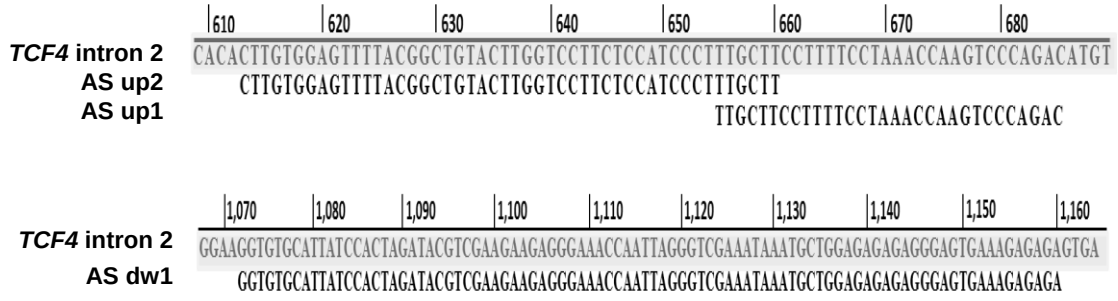

Supplementary Figure 1. Verification of *TCF4* antisense transcript by sequence-specific PCR in F35T patient-derived endothelial cells

(**A**) Scheme showing sequence-specific RT primers for cDNA generation and PCR primers.
(**B**) Sequences of primers for reverse transcription and PCR reactions.
(**C**) Image of PCR products after sequence-specific RT reaction for antisense transcript.
(**D**) Sanger sequencing of PCR amplicons.

A.

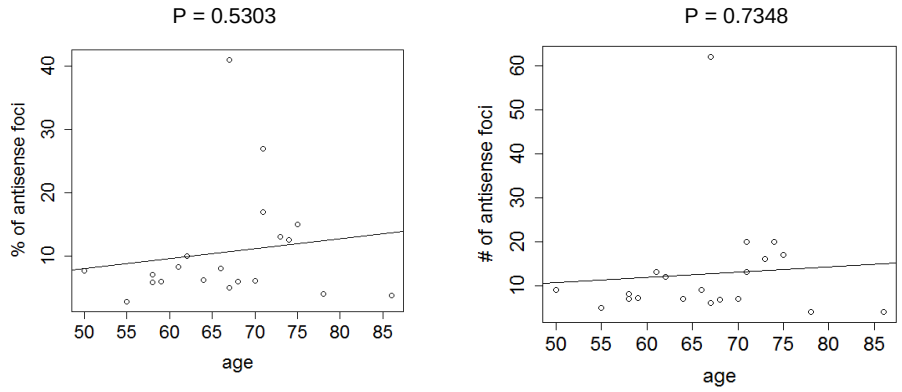

B.

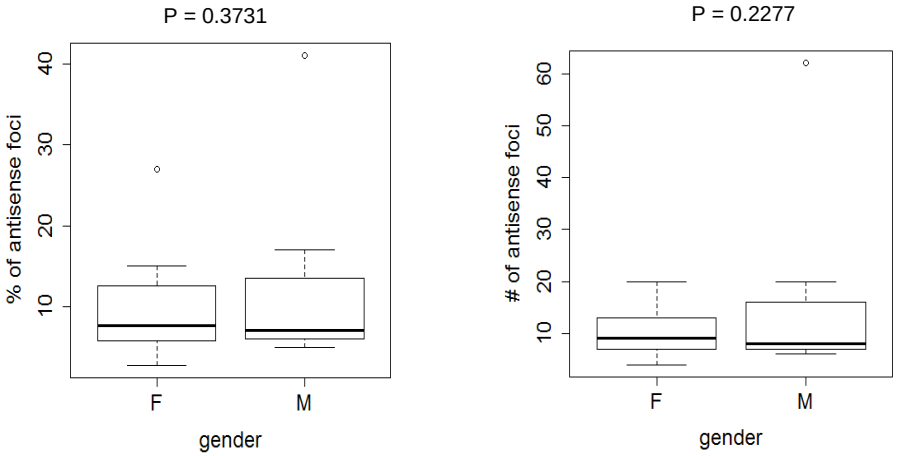

Supplementary Figure 2. Quantitative analysis of antisense foci in FECD patient corneal endothelial tissue samples.

(A) There is no significant correlation between antisense foci and patient age.

(B) Graphs showing that there is little correlation between antisense foci with patient sex.

A.

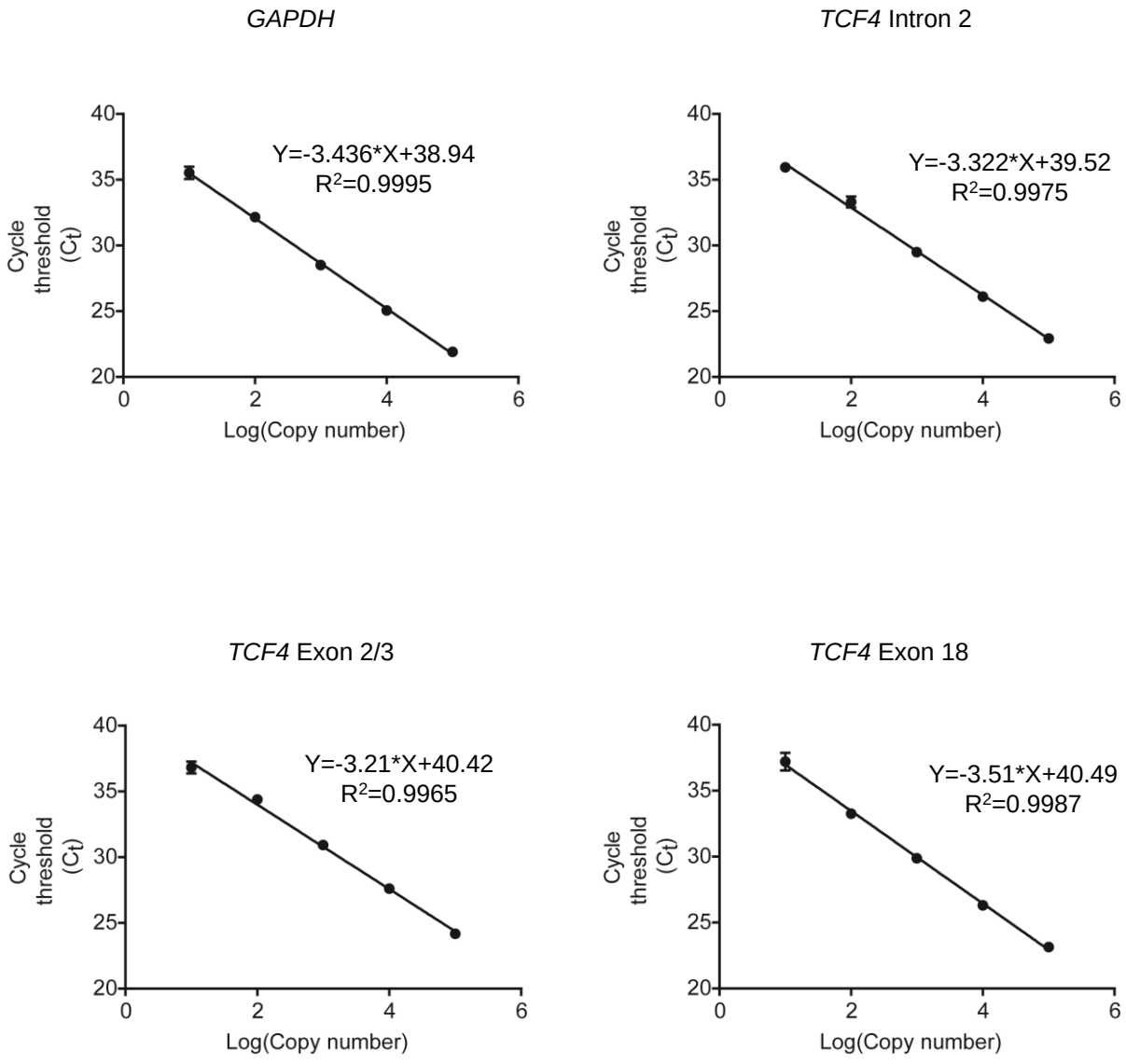

Supplementary Figure 3. Standard curve for qPCR efficiency of *GAPDH*, *TCF4* intron 2, *TCF4* exon 2/3, *TCF4* exon 18.

(**A**) A serial dilution of purified standard RNA, ranging from 10 to 10^5 copies was used to construct standard curve for qPCR efficiency by qPCR following reverse transcription. *Ct* value in each dilution were measured in triplicate.

A.

Tissue	Age	CTG repeat
Control tissue 1	71	13, 17
Control tissue 2	70	13, 19
Control tissue 3	63	16, 20
FECD tissue 1	66	17, 84
FECD tissue 2	50	12, 81
FECD tissue 3	72	33, 64

Supplementary Figure 4. Demographic data of endothelial tissues used for *TCF4* RNA copy number analysis.

A.

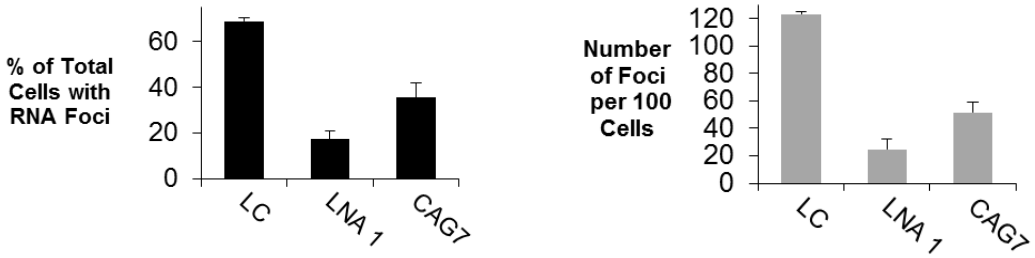

Supplementary Figure 5. Comparison of inhibition potency of CUG repeat-targeting antisense oligomers in F35T endothelial cell line.

(**A**) Effect on inhibition of CUG RNA foci by LNA 1, single-strand ASO CAG7(21-mer 2-OMe modified ASO).

A

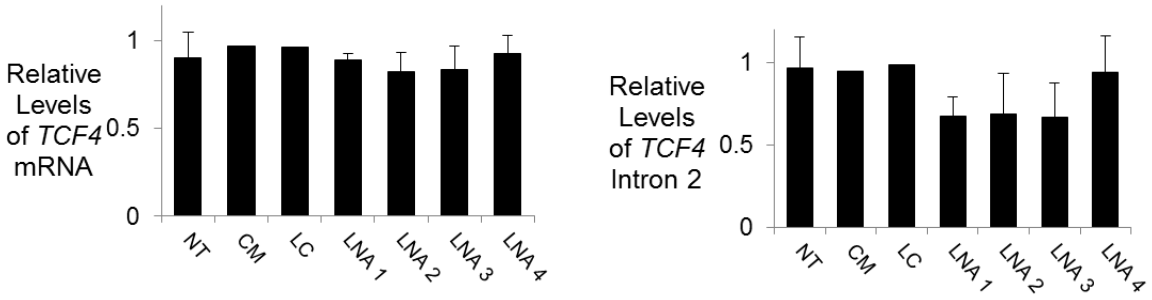

Supplementary Figure 6. Quantitative PCR showing that LNAs have little effect on *TCF4* mRNA and intron 2 RNA levels.

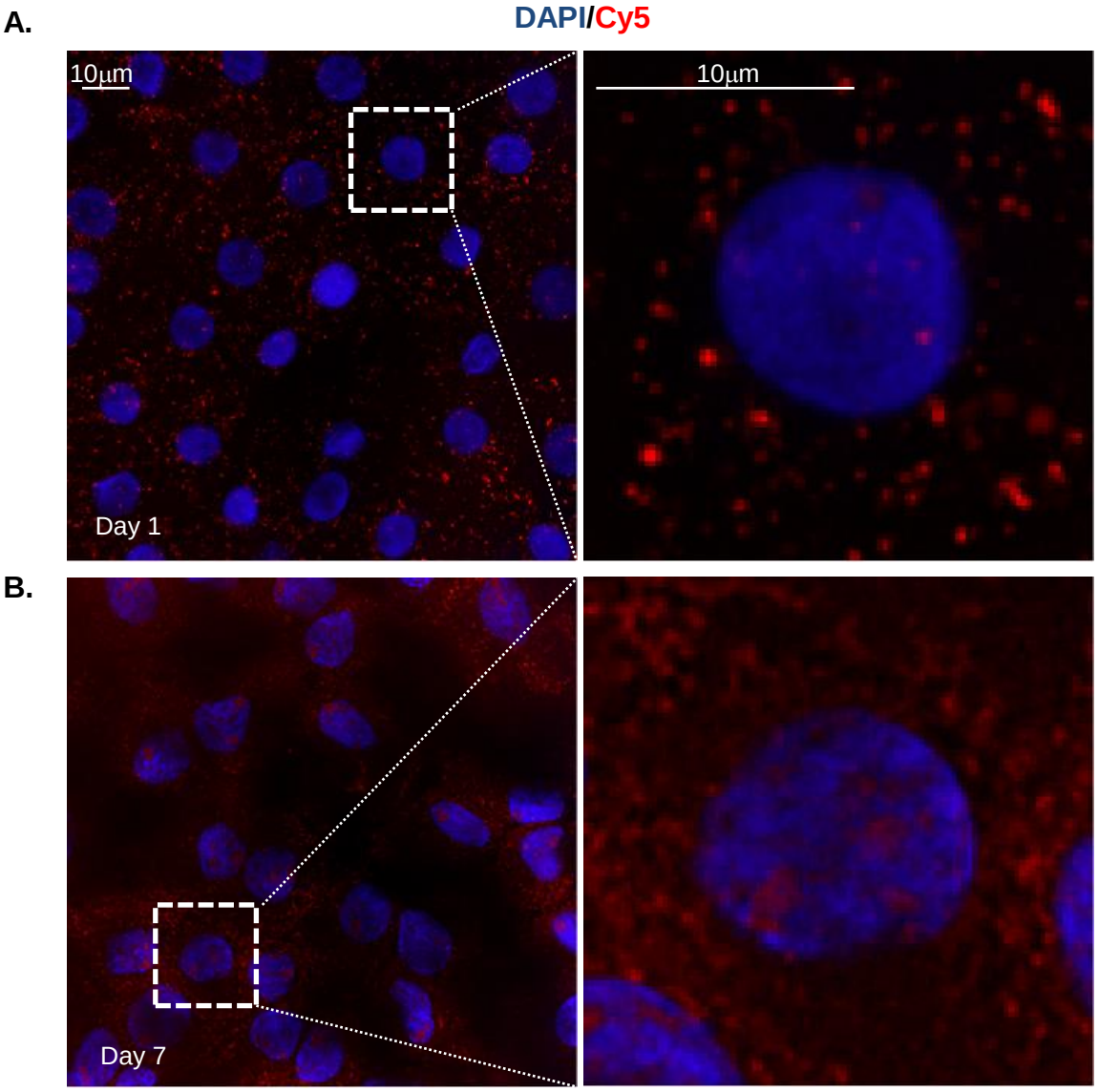

Supplementary Figure 7. Gymnotic delivery of single-strand ASO LC-Cy5 to *ex vivo* human corneas.

Fluorescent images of *ex vivo* corneal tissue treated with LC-Cy5 (10μM) for 1 day (**A**) or 7 days. (**B**). Uptake of oligonucleotides into the cytoplasm and the nucleus of endothelial cells is shown. The nuclei were stained with DAPI. The boxed region were enlarged and shown on the right. The cells were scanned from bottom to the top, about 15 slices of image were taken. Only the middle slices (start from 6 to 10) were used and Z-stacked to generate the pictures.

A.

Donor	Age	CTG Repeat
FECD Tissue 1	54	17, 110
FECD Tissue 2	51	13, 130
Control Tissue 1	55	13, 13
Control Tissue 2	64	13, 19

B. FECD Tissue 1 – Right Eye FECD Tissue 1 – Left Eye

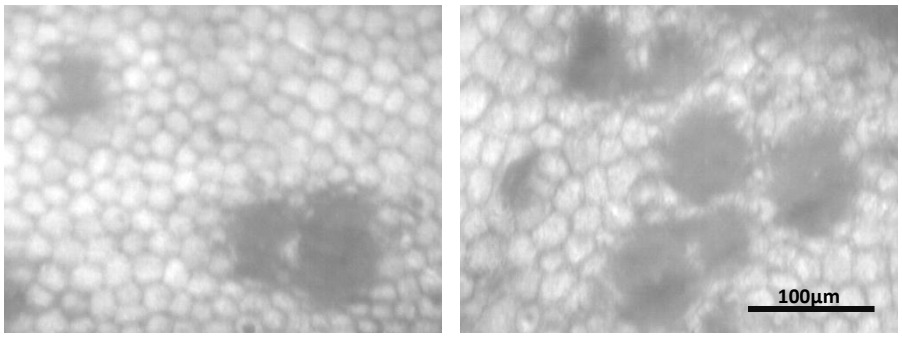

C. FECD Tissue 2 – Right Eye FECD Tissue 2 – Left Eye

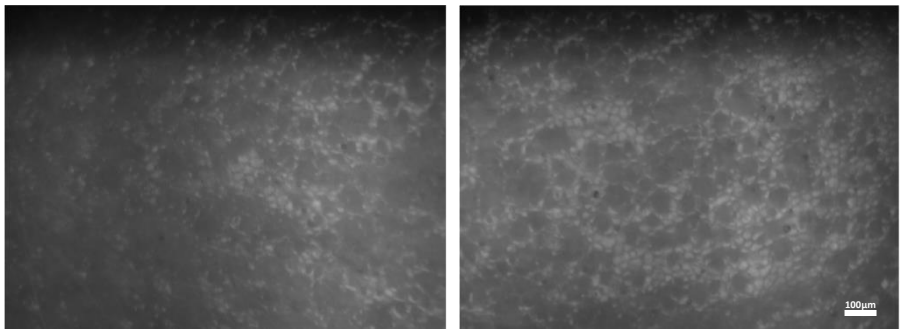

Supplementary Figure 8. Demographics data of *ex vivo* human corneas.
(**A**) Summary table of FECD-patient and control donors.
(**B**, **C**) Specular microscopy imaging of corneal endothelium. Dark spots correlate to focal excrescences (guttae) of Descemet's membrane, the basement membrane of the endothelium, which are diagnostic of FECD.